Published in final edited form as:
Plast Reconstr Surg. 2014 June ; 133(6): 1344–1353. doi:10.1097/PRS.0000000000000232.

Engineered Nasal Cartilage by Cell Homing: A Model for Augmentative and Reconstructive Rhinoplasty

Avital Mendelson, PhD[1,2], **Jeffrey M. Ahn, MD**[3], **Kamila Paluch, MS**[1,2], **Mildred C. Embree, PhD**[1], and **Jeremy J. Mao, DDS, PhD**[1,2]

[1]Columbia University Medical Center, Center for Craniofacial Regeneration (CCR), 630 W. 168 St. – PH7E, New York, NY 10032

[2]Departmental of Biomedical Engineering, Columbia University, New York, NY 10027

[3]Department of Otolaryngology-Head & Neck Surgery, Columbia University Medical Center, New York, NY 10032

Abstract

Current augmentative and reconstructive rhinoplasty surgeries utilize autologous tissue grafts or synthetic bioinert materials to repair nasal trauma or attain an aesthetic shape. Autologous grafts are associated with donor site trauma and morbidity. Synthetic materials are widely used but often yield an unnatural appearance and are prone to infection or dislocation. There is an acute clinical need for the generation of native tissues to serve as rhinoplasty grafts without the undesirable features that are associated with autologous grafts or current synthetic materials. Here, we developed a bioactive scaffold that not only recruited cells in the nasal dorsum *in vivo*, but also induced chondrogenesis of the recruited cells. Bilayered scaffolds were fabricated with alginate containing gelatin microspheres encapsulating cytokines atop a porous poly (lactic-co-glycolic acid) (PLGA) base. Gelatin microspheres were fabricated to contain recombinant human TGFβ3 at doses of 200, 500 or 1000 ng with PBS-loaded microspheres as a control. We first created a rat model of augmentation rhinoplasty by implanting bilayered scaffolds atop the native nasal cartilage surface that was scored to induce cell migration. Tissue formation and chondrogenesis in PLGA scaffolds were evaluated by image analysis and histological staining with Hematoxylin and Eosin, Toluidine Blue, Verhoeff Elastic-Van Geison, and aggrecan immunohistochemistry. Sustained release of increasing doses of TGFβ3 for up to the tested 10 wks promoted orthotopic cartilage-like tissue formation in a dose dependent manner. These findings represent the first attempt to engineer cartilage tissue by cell homing for rhinoplasty, and combine the advantage of autologous tissue formation by cytotactic factors embedded in a biomaterial scaffold that could potentially serve as an alternative material for augmentative and reconstructive rhinoplasty.

*Corresponding author: Jeremy J. Mao, Professor and Edwin S. Robinson Endowed Chair, Columbia University Medical Center, 630 W. 168 St. – PH7E, New York, NY 10032, Phone: 212-305-4475, jmao@columbia.edu.

Author contribution

A.M. designed and performed the experiments, assisted with surgical procedures, analyzed the data, and drafted the manuscript; J.A. performed the surgical procedures and assisted with data analysis; K.P. and M.E. assisted in experimental procedures; J.J.M. designed the experiments, analyzed the data and drafted the manuscript.

Financial Disclosure: None of the authors has a financial interest in any of the products, devices, or drugs mentioned in this manuscript.

Keywords

Stem cells; migration; rhinoplasty augmentation; cell homing; cytokines

Introduction

Reconstructive or augmentative rhinoplasty are surgical procedures to restore or alter nasal shape or projection. Autologous grafts are typically harvested from the nasal septum, outer ear or rib [1]. To create a nasal graft for reconstruction or augmentation, pieces of harvested cartilage are sometimes stacked and sutured together [2]. The graft is shaped such that the projecting end is wider than the proximal end, and is sutured in place at the caudal margin of the medial crura. An undesirable feature of autologous nasal grafting is the need for additional surgical procedures to harvest tissue, resulting in donor site trauma and morbidity [3, 4]. In addition, mechanical properties of rib cartilage are inferior to native nasal cartilage [5]. Another graft method involves the use of autologous fascia wrapped around diced autologous cartilage [6]. Although this method only requires a smaller source of autologous cartilage, harvesting autologous fascia increases the invasiveness of the procedure and obtaining a large enough volume of fascia is often challenging [6]. Allogeneic sources of cartilage circumvent the issue of donor site morbidity, but are difficult to obtain and require the patient to take long-term immunosuppressants to avoid graft rejections [1].

As an alternative to harvesting autologous cartilage, a number of synthetic implants are commercially available [4]. Medical grade silicone rubber has been widely used for nasal augmentation. Silicone is nonporous, can be shaped by the surgeon, and does not undergo enzymatic degradation. However, silicone does not integrate well with the surrounding tissue, and may extrude and result in chronic inflammation [7]. High-density polyethylene has also been extensively used for rhinoplasty. Polyethylene is flexible, easily carved and porous to allow tissue ingrowth and implant fixation. However, polyethylene augmentation is often unnatural in appearance and texture due to its high stiffness [7]. Lastly, polytetrafluoroethylene is a polymer with 30-μm pore size that allows limited tissue ingrowth, can be contoured and layered. Despite short-term favorable outcomes, long-term results suggest that polytetrafluoroethylene implants may be susceptible to infections and extrusion [5].

Despite the conceptual advantages of tissue-engineered nasal cartilage relative to autologous grafts or synthetic materials, few studies have attempted nasal cartilage regeneration to date [8–20]. Rabbit bone marrow precursor cells were expanded *in vitro* with TGFβ1 and wrapped around a nasal alar shaped poly(lactic-co-glycolic acid) (PLGA) scaffold, followed by implantation ectopically in the dorsum of nude mice for 4 weeks, resulting in positive cartilage markers [9]. Human nasal septum chondrocytes in fibrin were injected into the dorsal subcutaneous pocket of nude mice for 3 weeks and resulted in positive histological staining for chondrogenesis [10]. However, previous work on ectopic nasal cartilage regeneration invariably involved time-consuming and costly primary cell isolation and culture procedures, which carry the risk of immune rejection, pathogen transmission and possible mutagenesis [21]. Recently, we reported that host endogenous cells were recruited

by TGFβ3 and were responsible for the regeneration of an entire articular surface of a synovial joint [22]. We also showed that multiple stem/progenitor cell types could be recruited into a bioactive scaffold and chondrogenically differentiated *in vitro* with TGFβ3 [23]. The great majority of previous nasal cartilage regeneration studies have taken the approach of cell transplantation. The potential of cell homing as a tissue engineering method for rhinoplasty reconstruction or augmentation has not been investigated. We hypothesized that TGFβ3 would recruit cells around the nasal dorsum into the scaffold, followed by chondrogenic differentiation of the recruited cells. To this end, we developed a cell homing approach to promote the recruitment and chondrogenic differentiation of host endogenous cells into a bioactive, biomaterial-based scaffold that can be readily shaped for nasal reconstruction or augmentation.

Materials and Methods

Design and fabrication of the bioactive scaffolds

Bilayered scaffolds were fabricated with a top 2% w/v alginate layer containing gelatin microspheres encapsulating TGFβ3 and an underlying porous PLGA substrate (Fig. 1). Porous poly (lactic-co-glycolic acid) (PLGA) cylinders with varying polymer concentrations (10 – 40% wt/vol) were fabricated using salt leaching [24, 25]. Briefly, PLGA 50:50 crystals (Sigma, St. Louis, MO) weighing 1–4 g were dissolved in 30 mL dichloromethane. Dissolved PLGA solution was mixed with sodium chloride (Sigma, St. Louis, MO) that was sieved to ensure a particulate diameter between 150–500 μm. Solutions were created with a PLGA:NaCl weight ratio of 1:10, poured into a teflon coated 10-cm plate and allowed to air-dry overnight. Scaffolds were punched out of the PLGA sheet using a 6-mm diameter biopsy punch, salt leached with distilled water and dried using a lyophilizer. PLGA was selected as a scaffold due to its high porosity and a stiffness of approximately 200 MPa [26], representing a valid material for non-weight bearing nasal cartilage.

Gelatin microspheres were fabricated using a water-in-oil emulsion per our prior methods [23]. Briefly, gelatin solution (Sigma, St. Louis, MO) was dispersed in oil using a propeller and washed with acetone to remove residual oil. Microspheres were chemically cross-linked with 0.5% w/v glutaraldehyde and washed with 0.75% w/v glycine containing tween to block residual aldehyde groups on unreacted glutaraldehyde. Following lyophilization, gelatin microspheres were sterilized using ethylene oxide.

Microsphere aliquots (30 mg) were rehydrated in 30-μL phosphate-buffered saline (PBS) containing recombinant human TGFβ3 (Cell BioSciences, Santa Clara, CA) or PBS. At pH 7.4, the positively charged TGFβ3 was electrostatically bound to the negatively charged gelatin microspheres. TGFβ3 release profiles from gelatin microspheres were reported in our previous work [23]. PLGA discs were sterilized in 70% ethanol for 10 min and washed with distilled water. Sodium alginate (2% w/v, FMC BioPolymer, Philadelphia, PA) was mixed with 30 mg (dry wt) microspheres containing TGFβ3, dispensed onto a PLGA disk and cross-linked with calcium chloride. The total dimensions of the bi-layered bioscaffold were 6×4 mm (diameter×height).

Control conditions were tested to isolate the effects of cartilage scoring alone (Group 1) as well as to delineate the role of the cytokines in tissue formation from that of the biomaterials alone (Group 2). Groups 3–5 tested three different doses of TGFβ3 delivery (200 ng, 500 ng and 1000 ng) to determine the optimal dose that promotes cell migration and chondrogenesis. At the time of scaffold implantation, the native tip cartilage tissue was scored for all groups. Three rats were tested in each group and harvested after 10 wks for analysis of cell recruitment and chondrogenesis.

PLGA degradation characterization

PLGA degradation profiles were characterized to determine the optimal bulk concentration that promotes uniform degradation. PLGA discs were sterilized for 10 min in 70% ethanol with wet weights measured. PLGA disks were placed in each of 12-well tissue culture plates and submerged in 2-mL PBS containing 1% AB/AM followed by harvest after 0, 7, 17, 22, 27, 34 and 38 days and measurements of wet and dry weights. Scaffold morphology was examined at varying time points to observe internal pore structure using SEM.

Surgical implantation

Following IACUC approval, 10-month-old Sprague Dawley rats (Harlan, Indianapolis, IN) were anesthetized and maintained with 3–4% isoflurane (Fig. 2A). Lidocaine was administered subcutaneously and Carprofen was injected interperitoneally for pain relief. An incision was made on the head and the soft tissue was dissected down to the bone, forming a subcutaneous pocket (Fig. 2B). Scaffolds were positioned over the native nasal cartilage (Fig. 2B). However, due to the small size of the native cartilage relative to the size of the scaffold, half of the implant covered the native cartilage and the other half covered the native bone. The incision was sutured closed and one extra suture was placed over the top of the implant to secure it in place (Fig. 2C–D). Animals were sacrificed 10 weeks postoperatively. Harvested scaffolds were analyzed by gross morphology, histology and immunohistochemistry to evaluate cell recruitment and chondrogenesis.

Histological analysis of cell migration and chondrogenesis

Scaffolds were fixed in 10% buffered formalin, dehydrated, embedded in paraffin and sectioned at 5-μm thickness. Sections were chemically stained with hematoxylin and eosin (H&E), 0.1% toluidine blue (Sigma, St. Louis, MO), and modified Verhoeff Elastic-Van Gieson (Electron Microscopy Sciences, Hatfield, PA) to assess cartilage matrix formation, sulfated polysaccharides and elastic tissue fibers respectively.

For aggrecan immunohistochemistry, sections were blocked with peroxidase for 10 minutes to reduce background staining and digested with chondroitinase ABC (0.0015u/mL) for 60 minutes. Sections were subsequently incubated with primary antibody overnight at 4°C (10μg/mL, Millipore, Billerica, MA). After incubation with HRP polymer, sections were developed using AEC chromogen, due to a peroxidase catalyzed reaction with hydrogen peroxide. All sections were counterstained with hematoxylin and compared against a positive control of normal healthy rat nasal cartilage.

Statistical analysis

Quantitative data for each condition were pooled and upon confirmation of a normal data distribution, a one-way ANOVA with *post hoc* LSD test was used with a α value of $p \leq 0.05$.

Results

Scaffold Degradation Kinetics

A bilayered scaffold was fabricated with gelatin microsphere infused alginate gel atop a porous PLGA base (Fig. 1A–B). SEM images revealed high porosity among scaffolds fabricated with a 10%–40% PLGA concentration (Supp. Fig. 1). By day 7, PLGA underwent degradation with increased pore edge roughness (Supp. Fig. 1E–H). By day 27, the internal walls of PLGA scaffolds were engulfed with large pores (Supp. Fig. 1I–L). Pores of 30% and 40% PLGA scaffolds completely disintegrated by day 34 (Supp. Fig. 1M–P).

There was an inverse relationship between increasing PLGA concentrations and decreased degradation time (Fig. 1C–D). The degradation of 10% PLGA scaffolds was remarkably slow in comparison with 20%, 30% and 40% PLGA scaffolds. Scaffolds made with 20%–40% PLGA underwent surface degradation with a substantial decrease in total mass over time (Fig. 1C). Contrastingly, 10% PLGA scaffolds underwent bulk degradation with a relatively slow decrease in mass over time with some remaining structure at day 38 (Fig. 1C), whereas 40% PLGA scaffolds completely degraded by day 31 (Fig. 1D). At each tested time point, 20% PLGA scaffolds retained greater percent weight than 10% PLGA scaffolds and therefore was selected for use in all *in vivo* experiments.

Tissue and Histological Evaluation

To test *in situ* chondrogenesis by cell homing with an ultimate goal of rhinoplasty reconstruction and augmentation, 10%, 20% and 40% PLGA scaffolds with control-released TGFβ3 were implanted orthotopically on the surgically scored nasal cartilage in Sprague-Dawley rats with TGFβ3-free scaffolds and defect alone as control groups. Surgical scoring of the native tip cartilage was performed to expose resident stem/progenitor cells to TGFβ3 released from microspheres for recruitment into the porous PLGA base that was in direct contact with the scored nasal cartilage surface. Facial profile images taken immediately before and after scaffold implantation demonstrated that 20% PLGA scaffolds created an elevated nasal augmentation (Fig. 3). Following a 10-wk orthotopic implantation, facial profile images were taken immediately after animal euthanasia to reveal the level of augmentation visibly remaining (Fig. 4A–F). Additionally, ectopic tissue formation was imaged *in situ* (Fig. 4A′–F′) and after scaffold dissection to compare tissue size within groups (Fig. 4A″–F″). No visible ectopic tissue could be seen in Group 1, which only received cartilage scoring. Therefore, for this group perichondrium was isolated for use as a control to distinguish engineered tissue in other groups from native perichondrium tissue (Fig. 4A″). Group 2 control scaffolds displayed minimal ectopic tissue formation in two rats and no visible ectopic tissue formation in the third rat (Fig. 4B″). Increasing doses of TGFβ3 delivery induced an increase in tissue formation (Fig. 4C″, D″ and E″ respectively). Remarkable glistening white tissue formation could be seen due to the highest dose of

TGFβ3 delivery (Fig. 4E′). The combination of large ectopic tissue size and white tissue color set this group apart from all other groups. After tissue removal in Group 5 (Supp. Fig. 2A and B), the presence of a smooth underlying bone confirmed that the tissue formation was not causing negative pathology to the underlying bone (Supp. Fig. 2C). H & E staining of harvested scaffolds revealed no significant differences in tissue morphology between the perichondrium isolated in Group 1 (Fig. 5B) and the fibrous tissue isolated from the growth factor-free scaffolds used in Group 2 (Fig. 5C). Scaffolds in Groups 3–5 (Fig. 6A–C) however, had distinctly different tissue morphology compared to the Group 1 control (Fig. 5B). Chondrogenic differentiation was observed based on the presence of positive Toluidine Blue staining (Fig. 5D–E and 6D–E), Verhoeff Elastic-Van Gieson staining (Fig. 5G–I and 6G–I) and immunohistochemical staining for aggrecan (Fig. 5J–L and 6J–L). Control groups did not display any positive staining for toluidine blue among Group 1 (Fig. 5E) and minimal staining for Group 2 (Fig. 5F). Increasing levels of chondrogenesis was evident due to increasing doses of TGFβ3 delivery (Fig. 6D, E and F respectively). Chondrogenic differentiation was most prominent among Group 5 (Fig. 6F) tissue.

Bilayered Scaffolds Induce Chondrogenesis

The results of the toluidine blue staining were confirmed with the presence of positive aggrecan immunohistochemical staining (Fig. 5J–L and 6J–L). Minimal aggrecan staining was present among the control groups (Fig. 5K and L). Higher doses of TGFβ3 delivery (Fig. 6K–L) promoted enhanced aggrecan staining compared to lower delivery doses (Fig. 6J). Aggrecan staining was primarily located in the region surrounding the cytokine releasing microspheres (Fig. 6 J–L). This could be an indication that the cytokines were only able to diffuse a limited distance from the microspheres and promote chondrogenic differentiation in this region. Elastic cartilage formation was determined based on the presence of positive modified Verhoeff Elastic-Van Gieson staining (Fig. 5G–I and 6 G–I). Positive elastic cartilage formation was not evident in the control groups (Fig. 5H and I). Increased elastic cartilage staining was observed among Groups 4–5, which delivered a high-dose of TGFβ3 (Fig. 6H–I), compared to Group 3, which delivered a lower dose of TGFβ3 (Fig. 6G). In particular, positive elastic cartilage staining was concentrated around cytokine-releasing microspheres as observed by the aggrecan staining.

TGFβ3 alone was successful at inducing both cell homing and chondrogenesis with a dose dependent effect as indicated by immunohistochemical and chemical staining. Thus, as shown in a rat model, cells can be recruited into a predesigned bioscaffold and chondrogenically differentiated *in vivo*, representing a potential alternative therapy for rhinoplasty augmentation procedures.

Underlying bone does not display adverse effects from bioactive scaffold

Initially it was unknown if the high concentration of TGFβ3 locally released from Groups 3–5 would be toxic to surrounding cells and promote local tissue necrosis. However, after 10 weeks of implantation, visual inspection of the tissues surrounding the implant did not reveal any necrotic tissue (Supp. Fig. 2). Furthermore, after the implants were removed, the underlying bone surface appeared healthy (Supp. Fig. 2C). Therefore, high concentrations of locally released TGFβ3 do not appear toxic to surrounding tissues.

Discussion

Orthotopic cartilage-like tissue was engineered *in vivo* on the surface of native scored nasal cartilage using novel bioactive scaffolds with slow-releasing cytokines and without the use of cell transplantation. To our knowledge, this is the first attempt at applying cell homing approaches to engineer cartilage tissue for reconstructive and augmentative rhinoplasty. Visible alterations in nasal projection from engineered cartilage-like tissues of bioactive scaffold delivery group indicate the potential to capture endogenous cell sources by combining the advantage of autologous cell source with synthetic, biocompatible materials. This scaffold was designed with the possibility of a readily available off-the-shelf product. Since implant shape is a critical factor for reconstructive and augmentative rhinoplasty applications, PLGA was selected as the implant material for *in vivo* experiments because of its marked rigidity. In addition to creating a pronounced alteration of nasal shape, PLGA scaffolds promoted cell attachment and chondrogenic tissue formation. A major concern of current biomaterial-based implants for reconstructive and augmentative rhinoplasty is graft extrusion [4, 20]. Integration of the implanted bioactive PLGA scaffolds with the native tip cartilage indicates the potential to reduce for implant extrusion.

Cartilage scoring in the present work likely contributed to mobilization of resident stem/progenitor cells in the underlying native cartilage tissue. The approach was inspired by current orthopedic practice of microfracture to induce marrow bleeding and promote limited tissue repair [27, 28]. Gross examination of the harvested nasal tissue displays larger ectopic tissue formation amongst groups that received cartilage scoring compared to groups that did not receive cartilage scoring (data not shown). Histological analysis of harvested tissue revealed increased cartilage matrix as evident by Toluidine Blue staining amongst groups that received cartilage scoring (data not shown). Thus, cartilage scoring has a positive effect of increased tissue size and chondrogenic differentiation.

An important feature for reconstructive and augmentative rhinoplasty is the ability to tailor the graft to the individual patient [20]. Autologous grafts are stacked and sutured together in a bundle before implantation [2]. The bioactive PLGA scaffolds can be easily modified to create larger augmentations by varying the mold diameter used to create the PLGA scaffold base. For an off-the shelf product, three different scaffolds could be created with small, medium and large default sizes and easily trimmed for precise adjustments. Thus, the bioactive scaffold could potentially be used as a novel alternative implant design to current rhinoplasty treatment.

Supplementary Material

Refer to Web version on PubMed Central for supplementary material.

Acknowledgments

We would like to thank Dr. Kimi Kong and Dr. Mo Chen for their technical advice, and Ms. Fen Guo for technical assistance. The present study is funded in part by NIH grants RC2DE020767 and R01EB0062621.

References

1. Oseni A, Crowley C, Lowdell M, Birchall M, Butler PE, Seifalian AM. Advancing nasal reconstructive surgery: the application of tissue engineering technology. J Tissue Eng Regen Med.
2. Ahn J, Honrado C, Horn C. Combined silicone and cartilage implants: augmentation rhinoplasty in Asian patients. Arch Facial Plast Surg. 2004; 6(2):120–3. [PubMed: 15023800]
3. Quatela VC, Pearson JM. Management of the aging nose. Facial Plast Surg. 2009; 25(4):215–21. [PubMed: 19924594]
4. Sajjadian A, Naghshineh N, Rubinstein R. Current status of grafts and implants in rhinoplasty: Part II. Homologous grafts and allogenic implants. Plast Reconstr Surg. 125(3):99e–109e.
5. Jang YJ, Moon BJ. State of the art in augmentation rhinoplasty: implant or graft? Curr Opin Otolaryngol Head Neck Surg. 20(4):280–6. [PubMed: 22695624]
6. Jang YJ, Song HM, Yoon YJ, Sykes JM. Combined use of crushed cartilage and processed fascia lata for dorsal augmentation in rhinoplasty for Asians. Laryngoscope. 2009; 119(6):1088–92. [PubMed: 19418537]
7. Park SS. Fundamental principles in aesthetic rhinoplasty. Clin Exp Otorhinolaryngol. 4(2):55–66. [PubMed: 21716951]
8. Wolf F, Haug M, Farhadi J, Candrian C, Martin I, Barbero A. A low percentage of autologous serum can replace bovine serum to engineer human nasal cartilage. Eur Cell Mater. 2008; 15:1–10. [PubMed: 18247273]
9. Zhang J, Liu L, Gao Z, Li L, Feng X, Wu W, Ma Q, Cheng X, Chen F, Mao T. Novel approach to engineer implantable nasal alar cartilage employing marrow precursor cell sheet and biodegradable scaffold. J Oral Maxillofac Surg. 2009; 67(2):257–64. [PubMed: 19138597]
10. Vinatier C, Gauthier O, Masson M, Malard O, Moreau A, Fellah BH, Bilban M, Spaethe R, Daculsi G, Guicheux J. Nasal chondrocytes and fibrin sealant for cartilage tissue engineering. J Biomed Mater Res A. 2009; 89(1):176–85. [PubMed: 18431767]
11. Farhadi J, Fulco I, Miot S, Wirz D, Haug M, Dickinson SC, Hollander AP, Daniels AU, Pierer G, Heberer M, Martin I. Precultivation of engineered human nasal cartilage enhances the mechanical properties relevant for use in facial reconstructive surgery. Ann Surg. 2006; 244(6):978–85. discussion 985. [PubMed: 17122623]
12. Liu X, Sun H, Yan D, Zhang L, Lv X, Liu T, Zhang W, Liu W, Cao Y, Zhou G. In vivo ectopic chondrogenesis of BMSCs directed by mature chondrocytes. Biomaterials. 31(36):9406–14. [PubMed: 21056466]
13. Alexander TH, Sage AB, Chen AC, Schumacher BL, Shelton E, Masuda K, Sah RL, Watson D. Insulin-like growth factor-I and growth differentiation factor-5 promote the formation of tissue-engineered human nasal septal cartilage. Tissue Eng Part C Methods. 16(5):1213–21. [PubMed: 20178406]
14. Naumann A, Dennis JE, Aigner J, Coticchia J, Arnold J, Berghaus A, Kastenbauer ER, Caplan AI. Tissue engineering of autologous cartilage grafts in three-dimensional in vitro macroaggregate culture system. Tissue Eng. 2004; 10(11–12):1695–706. [PubMed: 15684678]
15. Dobratz EJ, Kim SW, Voglewede A, Park SS. Injectable cartilage: using alginate and human chondrocytes. Arch Facial Plast Surg. 2009; 11(1):40–7. [PubMed: 19153292]
16. Bichara DA, Zhao X, Hwang NS, Bodugoz-Senturk H, Yaremchuk MJ, Randolph MA, Muratoglu OK. Porous poly(vinyl alcohol)-alginate gel hybrid construct for neocartilage formation using human nasoseptal cells. J Surg Res. 163(2):331–6. [PubMed: 20538292]
17. Kita M, Hanasono MM, Mikulec AA, Pollard JD, Kadleck JM, Koch RJ. Growth and growth factor production by human nasal septal chondrocytes in serum-free media. Am J Rhinol. 2006; 20(5):489–95. [PubMed: 17063744]
18. Chang AA, Reuther MS, Briggs KK, Schumacher BL, Williams GM, Corr M, Sah RL, Watson D. In vivo implantation of tissue-engineered human nasal septal neocartilage constructs: a pilot study. Otolaryngol Head Neck Surg. 146(1):46–52. [PubMed: 22031592]
19. Han SK, Shin SH, Kang HJ, Kim WK. Augmentation rhinoplasty using injectable tissue-engineered soft tissue: a pilot study. Ann Plast Surg. 2006; 56(3):251–5. [PubMed: 16508353]

20. Watson D. Tissue engineering for rhinoplasty. Facial Plast Surg Clin North Am. 2009; 17(1):157–65. viii. [PubMed: 19181286]

21. Nie H, Lee CH, Tan J, Lu C, Mendelson A, Chen M, Embree MC, Kong K, Shah B, Wang S, Cho S, Mao JJ. Musculoskeletal tissue engineering by endogenous stem/progenitor cells. Cell Tissue Res. 347(3):665–76. [PubMed: 22382390]

22. Lee CH, Cook JL, Mendelson A, Moioli EK, Yao H, Mao JJ. Regeneration of the articular surface of the rabbit synovial joint by cell homing: a proof of concept study. Lancet. 376(9739):440–8. [PubMed: 20692530]

23. Mendelson A, Frank E, Allred C, Jones E, Chen M, Zhao W, Mao JJ. Chondrogenesis by Chemotactic Homing of Synovium, Bone Marrow and Adipose Stem Cells In Vitro. Faseb J. 2011

24. Yoshioka T, Kawazoe N, Tateishi T, Chen G. In vitro evaluation of biodegradation of poly(lactic-co-glycolic acid) sponges. Biomaterials. 2008; 29(24–25):3438–43. [PubMed: 18514306]

25. Lu L, Peter SJ, Lyman MD, Lai HL, Leite SM, Tamada JA, Uyama S, Vacanti JP, Langer R, Mikos AG. In vitro and in vivo degradation of porous poly(DL-lactic-co-glycolic acid) foams. Biomaterials. 2000; 21(18):1837–45. [PubMed: 10919687]

26. Mattioli-Belmonte M, Vozzi G, Kyriakidou K, Pulieri E, Lucarini G, Vinci B, Pugnaloni A, Biagini G, Ahluwalia A. Rapid-prototyped and salt-leached PLGA scaffolds condition cell morpho-functional behavior. J Biomed Mater Res A. 2008; 85(2):466–76. [PubMed: 17729257]

27. Sledge SL. Microfracture techniques in the treatment of osteochondral injuries. Clin Sports Med. 2001; 20(2):365–77. [PubMed: 11398363]

28. Bae DK, Yoon KH, Song SJ. Cartilage healing after microfracture in osteoarthritic knees. Arthroscopy. 2006; 22(4):367–74. [PubMed: 16581448]

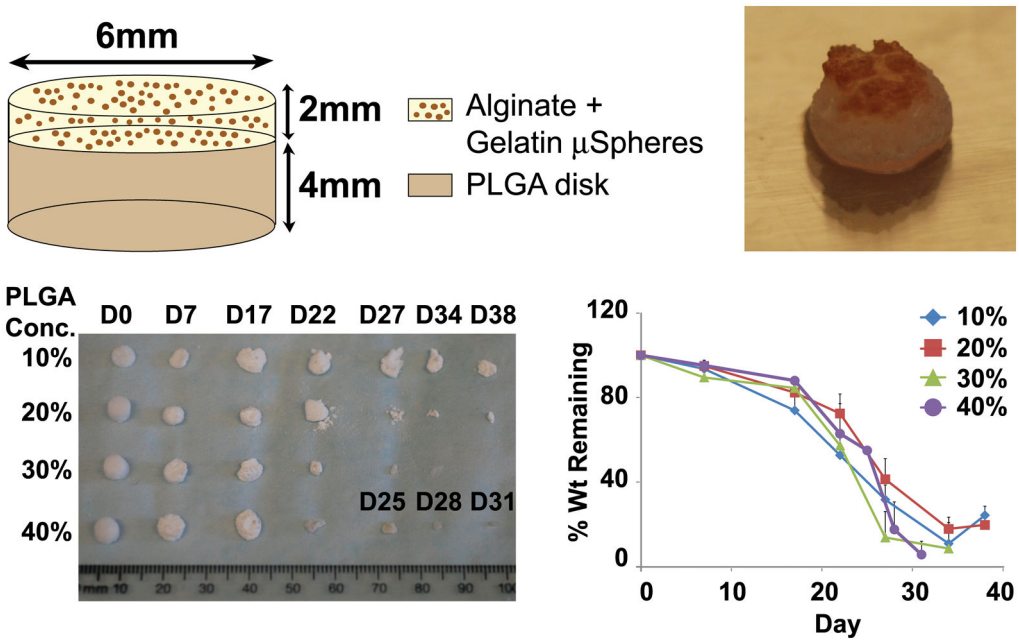

Figure 1.

PLGA scaffold schematic, gross image and degradation profile. (A) Schematic of bilayered implanted scaffolds. A top layer of alginate containing microspheres with slow releasing cytokines was situated over a base PLGA disk. (B) Gross image of scaffold before implantation. PLGA scaffolds with concentrations of 10%, 20%, 30% and 40% w/v were subjected to PBS culture for up to 38 days. After each time point, collected scaffolds were lyophilized and (C) imaged to observe scaffold structure. (D) Percent weight change over time was also calculated.

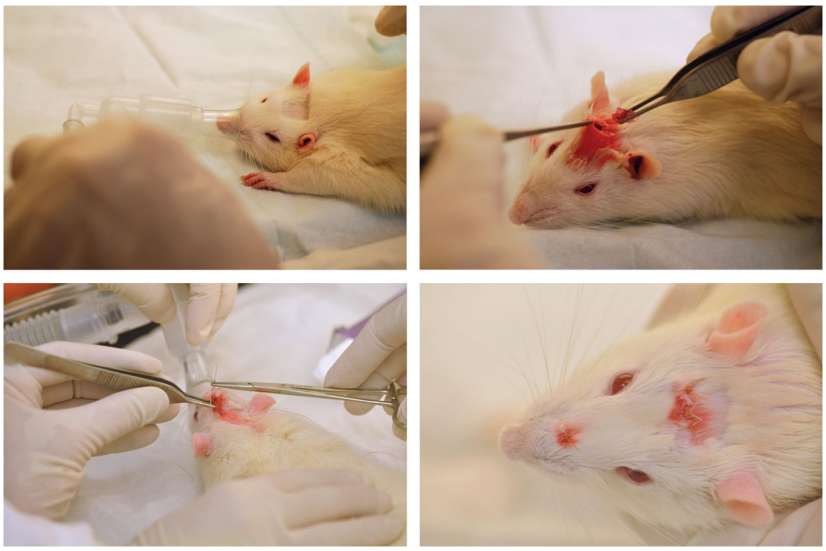

Figure 2.

Surgical methods used for scaffold implantation. (A) Rats were anesthetized and the surgical incision site was shaved. (B) An incision was created on the top of the head, followed by formation of a subcutaneous pocket leading to the nasal tip. Scaffolds were inserted into the pocket and onto the nasal tip. (C) Incision was sutured closed and an additional suture was placed above the implant to fix it in place. (D) Top-down view of finished surgery.

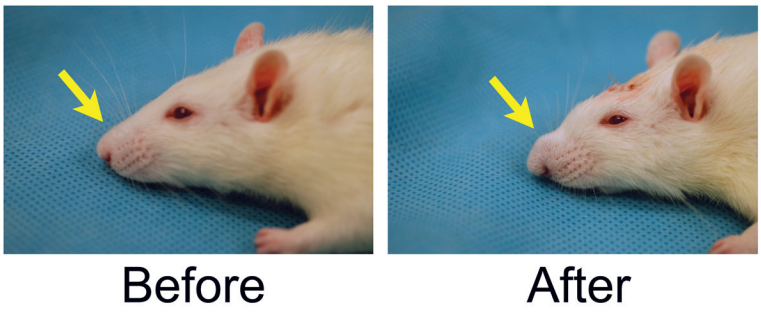

Figure 3.

Profile pictures of rhinoplasty augmentation before and immediately after surgery. Rat receiving Group 4 scaffold made from 20% PLGA containing 500ng of TGFβ3 is shown (A) before surgery and (B) after implantation.

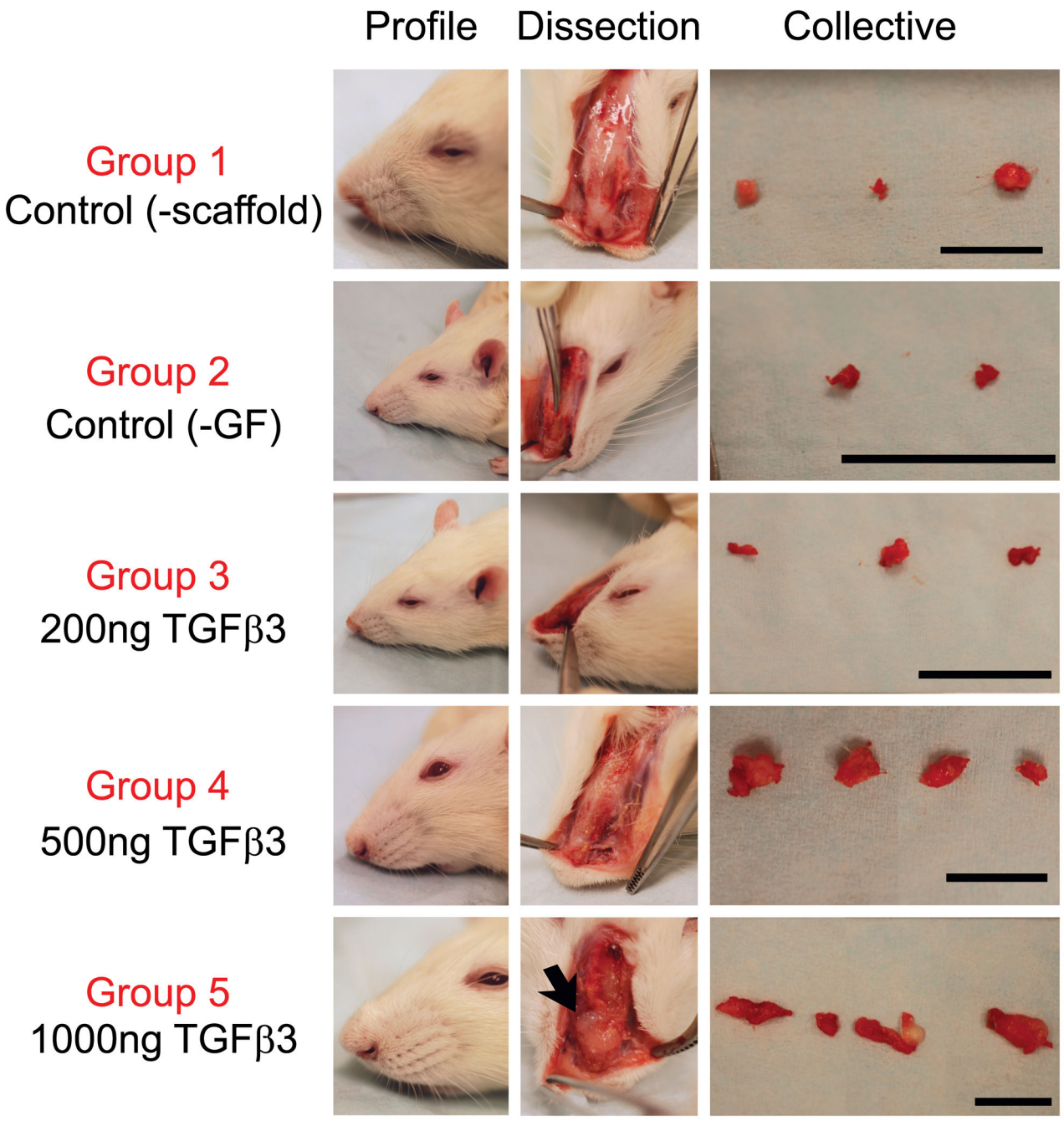

Figure 4.

Gross images of rhinoplasty harvests for groups 1–5. Profile images were taken immediately after harvest for visualization of remaining augmentation (A–F) and any ectopic tissue formation was dissected out (A′–F′). Harvested tissue from each rat in the experimental group was imaged together (A″–F″). Note: harvested tissue in D″, E″, and F″ consisted of two parts for some rats. Groups 1, 4 and 5: Scale = 1 cm. Groups 2 and 3: Scale = 1 inch

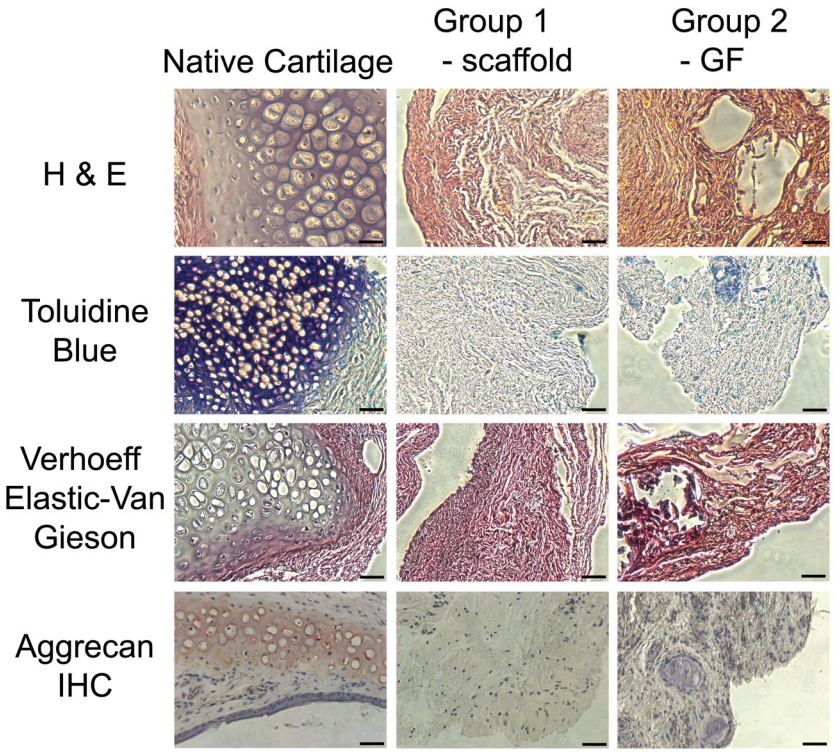

Figure 5.

Histological evaluation of control groups. Control groups 1 and 2 were stained with H & E (A–C), Toluidine Blue (D–E), modified Verhoeff Elastic-Van Gieson (G–I) and aggrecan immunohistochemistry (J–L) to assess cartilage matrix formation, sulfated polysaccharides, elastic tissue fibers, and aggrecan matrix protein respectively. Scale = 50μm.

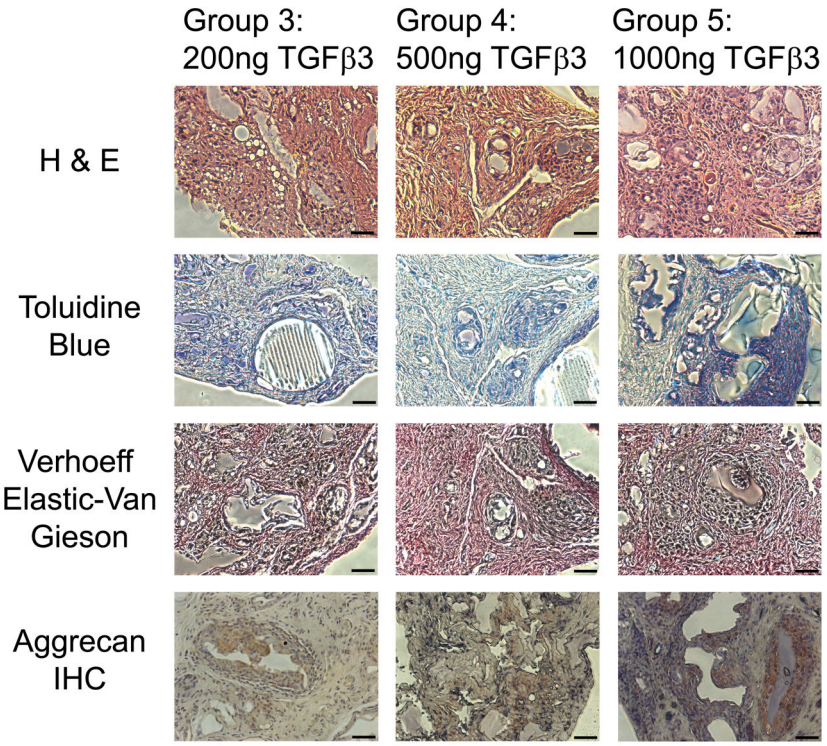

Figure 6.

Histological evaluation of experimental groups. Experimental groups 3, 4 and 5 were stained with H & E (A–C), Toluidine Blue (D–E), modified Verhoeff Elastic-Van Gieson (G–I) and aggrecan immunohistochemistry (J–L) to assess cartilage matrix formation, sulfated polysaccharides, elastic tissue fibers, and aggrecan matrix protein respectively. Scale = 50μm.

Table 1

Experimental design and scaffold conditions.

Group 1	Control: Cartilage Scoring
Group 2	Control: Scaffold − GFs + Cartilage Scoring
Group 3	Scaffold + 200ng TGFβ3 + Cartilage Scoring
Group 4	Scaffold + 500ng TGFβ3 + Cartilage Scoring
Group 5	Scaffold + 1000ng TGFβ3 + Cartilage Scoring